Breast Enhanced Scintigraphy Testing Distinguishes Between Normal, Inflammatory Breast Changes, and Breast Cancer: A Prospective Analysis and Comparison With Mammography

Richard M. Fleming, MD, FICA, FACA, FASNC, FACP, and William C. Dooley, MD, FACS

PLEASE PROVIDE AN ABSTRACT OF NO MORE THAN 175 WORDS AND 4 TO 5 KEY WORDS

In 1995, approximately 257,000 cases of cancer were diagnosed in the United States, with nearly 72,000 cases of breast cancer accounting for nearly 20,000 deaths.[1] By 1999, this number had risen to more than 600,000 cases of cancer, of which more than 175,000 were cases of breast cancer, which accounted for some 43,300 deaths.[2] The ability to detect and treat breast cancer is dependent on monthly breast self-examinations, physician breast exams, mammography, and most recently magnetic resonance imaging and breast scintigraphy. Concerns over false-negative and false-positive mammograms and their effects on women and their families have emphasized the need to improve the accuracy of detecting breast cancer.[3-6] Scintigraphy imaging for heart disease and cancers has been employed for decades, and with the development of technetium compounds,[7] the accuracy of detecting each has increased significantly.

Considerable research has demonstrated that resting sestamibi (technetium-99m hexakis 2-methoxyisobutylisonitrile [Miraluma]) imaging of the breast without quantification has sensitivity and specificity comparable to mammography for the detection of breast cancer.[8-15] This approach is referred to as resting, since the study is performed while the patient is resting on a table without any efforts to enhance or change blood flow. Additional research has shown that technetium-labeled compounds can also be used to evaluate lymph nodes, including sentinel node staging of breast cancer.[16-18]

In early 1999, 10 women with a history of heart disease and abnormal mammograms were initially imaged using standard resting (Miraluma) protocols. These same women were then studied less than 1 week later[19] to search for evidence of heart disease prior to breast biopsies using high-dose dipyridamole (HDD) imaging following a protocol we have previously reported in the literature.[20-22] HDD causes vasodilation of blood vessels and enhanced delivery of the isotope. It works via the release of endogenous adenosine from vascular endothelial cells. When these cells are normal (i.e., not diseased/dysfunctional), the blood vessels dilate, subsequently carrying more blood and isotope. This approach has been shown to increase the accuracy of detecting heart disease without reducing coronary blood flow or precipitating myocardial injury.[20-22]

In an effort to determine whether simultaneous imaging of the breast and heart could be performed in these women, we compared the 2 studies (breast and heart) and determined that breast imaging, which requires 925 to 1110 MBq, could be incorporated into the cardiac study immediately after pharmacologic stress (HDD) was completed. This approach allowed for equal amounts of sestamibi to be given in both the resting (Miraluma) study and the post-HDD condition so that a tête-à-tête **PLEASE REWORD "TÊTE-À-TÊTE"** comparison of the 2 breast images could be made. When these initial studies were compared, significantly greater isotope activity was seen in the post-HDD studies in regions of inflammatory changes of the breast and cases of breast cancer. No significant differences occurred in the normal breast images.

RMF is at the Camelot Foundation, Omaha, Nebraska. WCD is at the Oklahoma University Health Science Center, Oklahoma City.

Correspondence: Richard M. Fleming, Camelot Foundation, 9290 West Dodge Road, Suite 204, Omaha, NE 68114. Email: rfmd1@fhhi.omhcoxmail.com.

The breast-imaging component following HDD infusion was later named the breast enhanced scintigraphy test (BEST), since isotope delivery to the breast was enhanced following HDD-induced vasodilation.[20-22] Further enhancement of the image resulted from displaying the results in a blue-green color format (instead of black and white), thereby eliminating false positives reported when reading black-and-white resting (Miraluma) images and making it easier to identify regions of greatest isotope activity.

To further evaluate BEST imaging, 100 women were prospectively studied and the following questions were asked: (1) What is the sensitivity (ability to detect the presence of disease when present) and specificity (the ability to detect the absence of disease when absent) of BEST imaging in detecting breast cancer? (2) How does BEST imaging compare with the results of mammographic detection of breast cancer? (3) Can BEST imaging be used to distinguish more than just the presence or absence of cancer (i.e., is there a quantitative maximal count activity [MCA] following BEST imaging that distinguishes between normal breast tissue, inflammatory changes of the breast, and breast cancer)?

Methods

Subject Enrollment

One hundred women were studied from February 1999 to February 2001, ranging in age from 27 to 88 years. Women were enrolled in the study if they had an abnormal mammogram (58) and/or a palpable mass (3) or expressed an interest in participating in a breast cancer detection study. Women were excluded from the study if they were pregnant or breastfeeding. Subjects underwent mammography and signed institutional consent forms prior to BEST imaging and/or surgical procedures. Mammography and BEST imaging were completed within 2 weeks of each other.

BEST

Each woman was studied in the fasting state, with emphasis on avoiding caffeine prior to the study, which would inhibit the vasodilatory character of HDD. An intravenous catheter was placed in the right arm unless there was concern about a mass in the right breast, in which case the catheter was placed in the contralateral (left) arm. Patients were placed in the supine position, and the intravenous catheter was connected to intravenous tubing, through which HDD and sestamibi were delivered. Dipyridamole was infused during the first 4 minutes of the study.[20-22] Two minutes later, 925 to 1110 MBq of sestamibi was infused. Continuous monitoring of the electrocardiogram was performed in addition to blood pressure monitoring every 2 minutes.

Breast imaging begins with the patient placed in a prone position on a padded surface with removable padding inserts. This allows each breast to be positioned independently through the padding in a comfortable position once the padding inserts are removed. As shown in Figure 1, planar breast imaging then begins, first with one breast (BrQL) and then the other (BrCL). Patients are then placed on their back for the anterior (BrAS) image of both breasts. Areas of special concern (BrQ1, BrQ2) are then studied in the prone position. This technique requires no breast compression. The total time from the beginning of the procedure to the completion of breast imaging can be up to 60 minutes, although breast imaging typically requires 30 minutes following the HDD infusion.

Breast image acquisition and reconstruction were performed using a Siemens orbiter single photon emission computed tomography camera with 75 photomultiplier tubes and a 128 by 128 matrix. The images are acquired with the camera head in a stationary (planar) position. The camera, computer, and software providing quantification of MCA were supplied by NC Systems (Boulder, CO). A low-energy, high-resolution collimator was used, which had a resolution of 3.4 mm.

Interpretation of BEST Imaging Results

Images were reconstructed using the NC Systems software. Following reconstruction, images were displayed initially in black and white and then converted into a blue-green format for interpretation, as shown in Figure 2. The blue-green image format was used to determine whether an abnormality was present or absent in either breast. An example of the appearance of normal breast tissue, inflammatory breast changes, and breast cancer is shown in Figure 2.

Following the image reconstruction and presentation of each breast image, the region of greatest MCA was determined and quantified. This assessment of MCA was performed using computer assessment of MCA as measured and displayed on the computer monitor. All readings and determination of MCA were determined for each breast prior to any knowledge of clinical, mammographic, or pathologic information that could in any way bias the results. These procedures were performed at a recognized center of excellence for nuclear procedures under the direct supervision of a physician boarded in nuclear imaging.

Mammography

Subjects underwent mammography using conventional cephalocaudal and medial-lateral oblique pro-

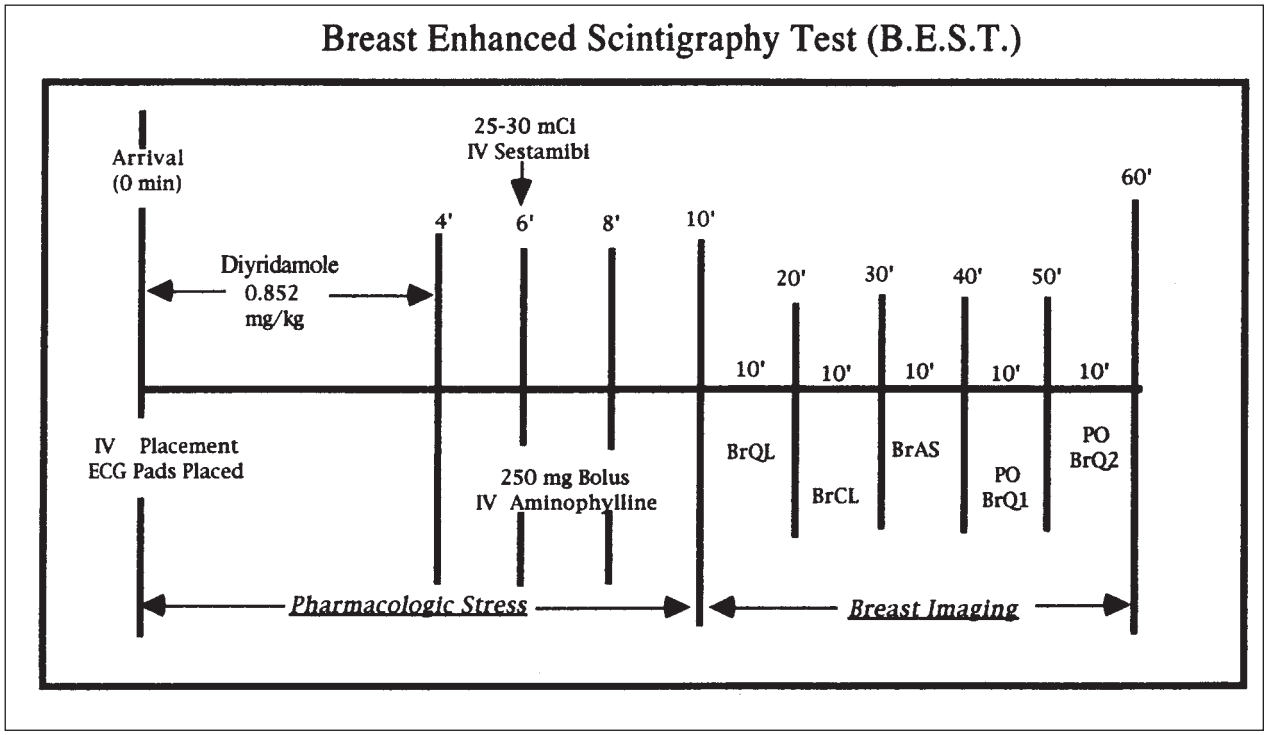

Figure 1 Sequence of imaging following the breast enhanced scintigraphy test (BEST) protocol. The BEST procedure is performed beginning with the placement of an intravenous catheter in the right antebrachium, or the left antebrachium if there is a specific question with regard to cancer in the right breast. The study is divided into the pharmacologic stress component, where dipyridamole is used to enhance blood flow and tracer delivery to the breasts, and the breast imaging component, where planar images of the breasts are acquired. The imaging sequence consists of BrQL (lateral view of breast in question or the right breast if neither breast is specifically suspected of having an abnormality), BrCL (lateral view of the breast contralateral to BrQL), BrAS (anterior view of breasts), PO BrQ1 (posterior oblique view of first breast noted to have abnormal activity on initial views), and PO BrQ2 (posterior oblique view of the other breast if its activity is abnormal).

jections. Trained and boarded radiologists who routinely perform mammography services and were considered experts by their peers interpreted results. These results were later compared with the results obtained from BEST imaging and biopsy results.

Tissue Specimens

Following the diagnostic studies (mammography and BEST imaging), biopsies were performed on 60 of the 100 women. These biopsies were performed by needle biopsy, open biopsy, or when possible by endoscopic visualization of breast tumors[23] (ductoscopy). Biopsies were performed on those women who had an abnormal mammogram suspicious for breast cancer, an abnormal BEST image, or a palpable mass on initial referring physician physical examination. Biopsies were not performed on women with both a normal mammogram and a normal BEST image. Examples of ductoscopy images are shown in Figure 2, including examples of normal, inflammation, and breast cancer. These results match results obtained from BEST imaging, as shown in Figure 2. The results of pathology specimens were then compared with the results obtained by mammography and BEST imaging.

Statistical Analysis

Outcomes were based on pathologic information obtained from surgical specimens acquired following diagnostic studies. The sensitivity and specificity for both mammography and BEST imaging were then determined. MCA from BEST images was determined for each breast and compared with the results of surgical specimens. Mean ± standard deviation, confidence intervals, and other descriptive statistics were then determined for normal breast tissue, inflammatory breast changes, and breast cancer. Differences in MCA between these 3 groups were then compared using a 2-tailed *t* test analysis in addition to a simple linear regression of MCA.

Results

One hundred women, including 91 Caucasians, 5 Hispanics, 2 African Americans, and 2 women of Mediterranean origin, ranging in age from 29 to 88 years (51 ± 11) were studied over a 2-year period of time using mammography and BEST imaging to determine whether they had breast cancer. No differences in outcomes were found based on age or race.

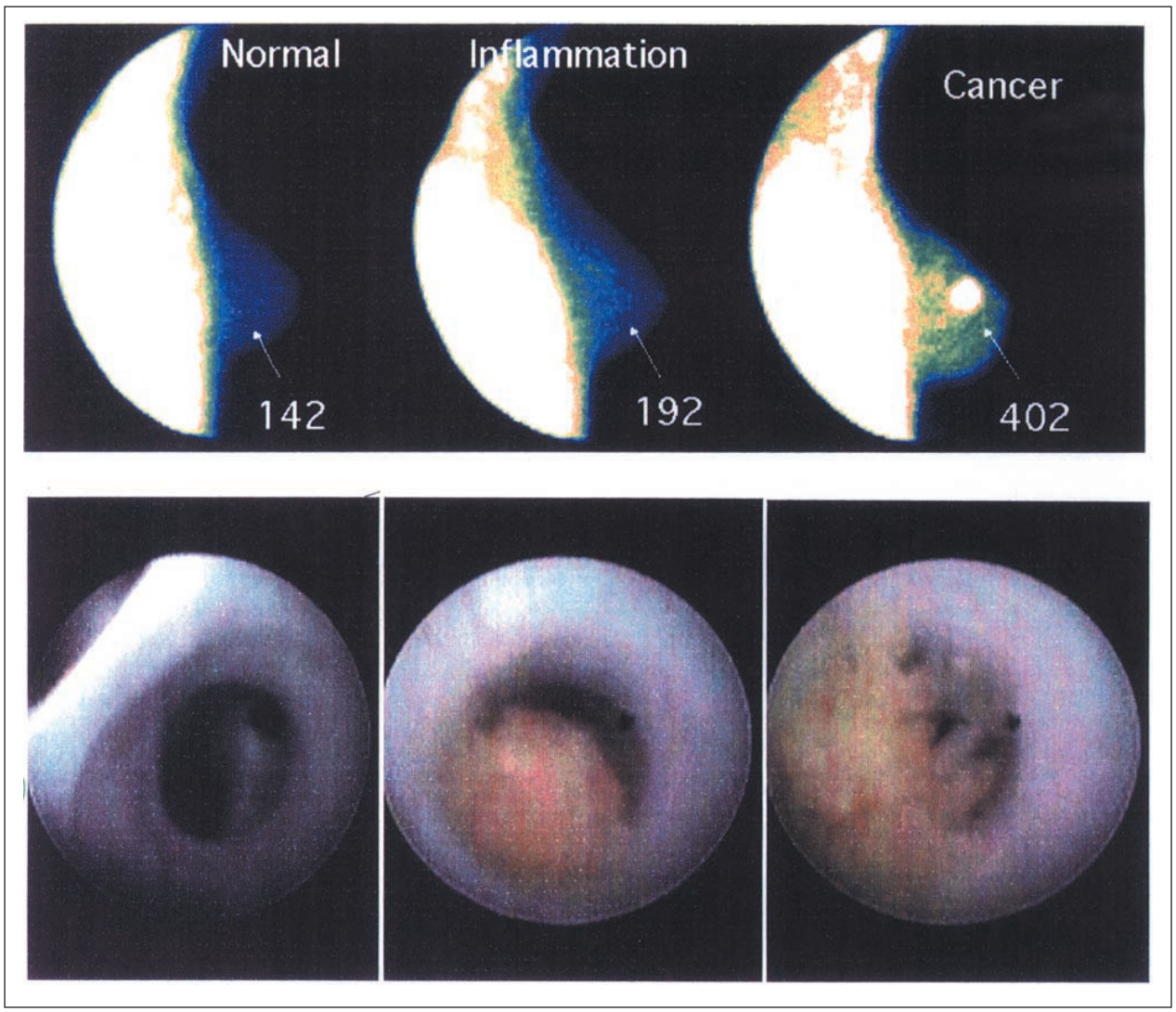

Figure 2 Examples of normal, inflammation, and breast cancer. In the top row are 3 lateral projections obtained showing normal, inflammation, and breast cancer. Each image is displayed in the blue-green color format with regions of maximal activity determined by computer analysis of each breast. The region of maximal activity for the normal breast was 142, whereas the region of greatest activity in the breast with inflammation was 192. The breast with breast cancer had a maximal count activity of 402. Breast cancers as small as 4 mm can be identified by this method. In the second row of images, there is an example of normal (far left), inflammatory breast changes (middle), and breast cancer (far right) as seen using ductoscopy to identify these same regions.

Based on the biopsy specimens, breast cancer was present in 8% (16 of 200) and inflammatory changes (e.g., fibrocystic disease) were present in 43.5% (87 of 200) of the breast images. The remaining 48.5% (97 of 200) were normal. Assuming that each of the 40 nonbiopsied women had "truly" normal breasts without cancer, then mammography demonstrated a sensitivity and specificity of 69% and 84% compared with 100% for BEST in the detection of breast cancer. Mammography and BEST imaging agreed 76% of the time with regard to the presence or absence of cancer. In 5 of the 16 cases of breast cancer, the mammogram failed to detect the cancer that was discovered by BEST imaging. Excluding those women who did not undergo biopsies who had normal-appearing mammograms and BEST imaging studies, the sensitivity and specificity of mammography were 68.7% and 66%, respectively, whereas BEST imaging continued to have 100% sensitivity and specificity.

The descriptive statistics for MCA outcomes for each of the 3 (normal, inflammatory breast changes, and breast cancer) groups are shown in Figure 3. The MCA in normal breast tissue was 144 ± 30 with a 95% confidence interval (CI) of 138 to 150. The MCA in normal breast tissue was 209 counts. Inflammatory breast tissue had an MCA of 229 ± 50, whereas breast cancer MCA was 446 ± 80. The 95% CI for inflammatory changes of the breast ranged from 219 to 240, whereas the 95% CI for breast cancer ranged from 404 to 489.

Figure 4 represents the graphical depiction of MCA for each of the 3 groups. The graph displays the median activity seen in each of the 3 groups, along with minimal and maximum activity measured. Figure 4 also displays confidence data. The results of 2-tailed *t* test analysis demonstrated statistically significant differences between normal and inflammatory MCA ($P \leq .001$), between inflammatory and breast cancer MCA ($P \leq .001$), and between normal and breast cancer MCA ($P \leq .001$). Regression analysis demonstrated a high correlation of 0.84 between the MCA and changes in the breast.

Discussion

Breast cancer is the second (heart disease is number one) leading cause of death among U.S. women,[24] with 1 in 8 women developing breast cancer in their lifetime. Prior efforts to increase the diagnostic accuracy of detecting breast cancer have had some, but limited, success. Similar limitations existed in the detection of heart disease using exercise stress and thallium-201 imaging; however, using a different group of isotopes (e.g., sestamibi) and combining these with pharmacologic stress (e.g., HDD)[20,21,25] agents resulted in improved detection of coronary artery disease. Efforts to apply sestamibi imaging to the detection of breast cancer have primarily used resting (Miraluma) studies to search for increased mitochondrial activity typical of cancers. However, these resting studies yielded results equivalent to mammography and provided little additional information.

Our initial efforts to combine the evaluation of breast cancer and heart disease imaging were possible by combining the 2 studies and imaging the breasts after the administration of the recommended 925 to 1110 MBq of sestamibi. To do these 2 tests simultaneously[26] required that the breast imaging follow HDD pharmacologic stress as shown in Figure 1. The initial studies demonstrated a greater count activity in the breast tissue in regions of inflammation, cellular atypia, and cancer than was seen during resting studies[26] of the same individuals given the same amount of isotope.

This increased uptake in regions of inflammatory changes and abnormal breast cancer tissue, but not in regions of normal breast tissue, is consistent with the increased blood supply expected from (1) increased blood supply in regions of inflammation, as the body is responding to the inflammation, and (2) the increased vascularity of tumors. These changes when quantified for MCA demonstrated statistically significant differences between normal, inflammatory breast changes, and breast cancer. This increased MCA is a reflection of the number of mitochondria present *and* the vascularity of the site. Hence, the detection of MCA less than 210 reflected normal breast tissue without increased vascularity or increased mitochondrial activity. This would clearly be different in lactiferous breasts and would require that breastfeeding and milk production return to baseline levels before BEST imaging is scheduled, not only for the purpose of study accuracy but also for the safety of the baby.

Increased MCA between 130 and 320 is seen in breasts with inflammatory changes. This increased activity is the result of increased vascularity secondary to the inflammatory response and the increased mitochondrial activity present with leukocytes, monocytes, and so on when compared with normal breast tissue. The ability to distinguish these inflammatory sites from normal breast tissue is dependent on the presentation of breast images in the blue-green color format. The initial computer presentation of images in black and white[26] demonstrated false-positive artifacts also reported in Miraluma studies. Visual discernment by the human retina is optimized in the yellow-green part of the color spectrum. The display of images in the blue-green color format should theoretically result in enhanced detectability of normal and abnormal image appearance. The overlap between normal and inflammatory changes is perhaps less important, since neither represents, nor is confused with, breast cancer.

Although some experts may agree to disagree about whether all anaplastic, dysplastic, or metaplastic cells will become "cancers," it has been clearly shown that cancers are dependent on their blood supply to maintain their growth and viability. Similarly, the heart requires a certain amount of blood supply to meet its needs and when coronary artery disease is sufficiently advanced to result in angina,[20,21,27] neovascularization/angiogenesis may occur following the release of any of a number of vascular growth factors.[27] These same growth factors are released from cancers,[28,29] providing increased blood supply (neovascularization/angiogenesis) to the cancer. Thus, the increased vascularity associated with cancers allows HDD to further increase delivery of the isotope to the cancer until MCA exceeds 270. Lesions with MCA from 270 to 320 may represent early cancers, which are increasing their angiogenic factors and subsequent blood supply. This is perhaps the earliest diagnostic marker that a lesion will become a cancer unless removed, since these cells have transitioned from cells that had produced more vascular inhibitory factors to cells with more stimulatory factors for angiogenesis. The use of BEST imaging can identify abnormalities as small as 4 mm in size.

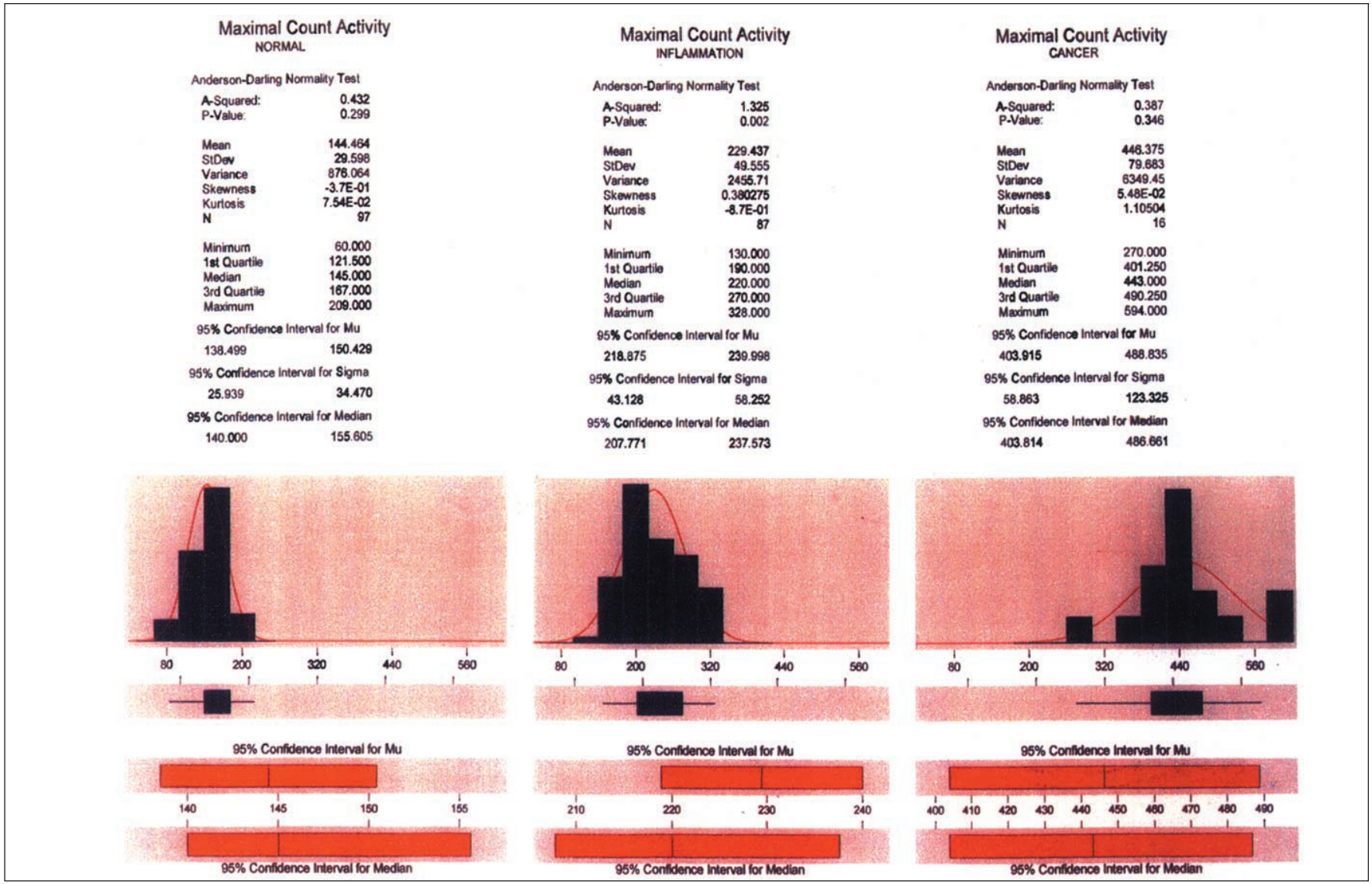

Figure 3 Statistical analysis of maximal count activity for normal, inflammatory changes of the breast, and breast cancer. Descriptive statistical analysis for normal, inflammatory changes of the breast, and breast cancer are displayed side-by-side including (bottom panel) a frequency distribution curve of maximal count activity with confidence intervals. The complete descriptive statistics for each group are shown above the frequency distribution curves.

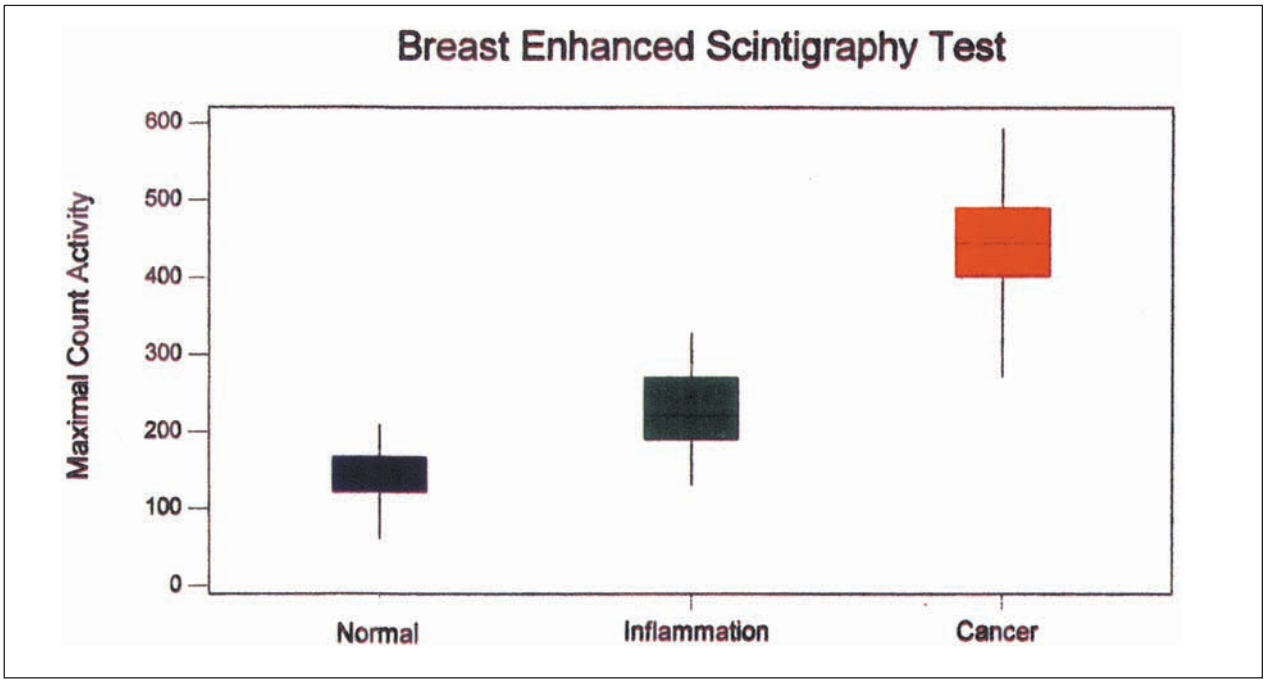

Figure 4 Maximal count activity for normal, inflammatory breast changes, and breast cancer as measured by breast enhanced scintigraphy testing. The blue rectangle represents the maximal count activity seen in normal breast tissue, whereas the green rectangle represents maximal count activity of inflammatory breast changes and the red rectangle represents maximal count activity for breast cancer. The rectangular regions represent the median values ± first and third quartiles. The vertical bars projecting above and below the rectangular box plots represent the minimum and maximum values reported.

Conclusion

The true enhancement of the BEST is a 4-fold process that takes advantage of the increased mitochondrial activity and angiogenesis present in inflammatory and cancerous states. First, the use of a low-energy, high-resolution collimator increases the resolution and allows for the detection of lesions as small as 4 mm in diameter. Second, the enhanced delivery of isotope through augmentation of blood flow following the administration of HDD takes advantage of increased blood supply resulting from either inflammatory increases in blood supply or angiogenesis resulting from tumor angiogenic factors, neither of which is seen in normal breast tissue. Third, the presentation of images in the blue-green color format improves reader interpretation of abnormal regions, eliminating false positives. The fourth and final component is the quantification of MCA guided by the blue-green image of the breast. This technique requires a quantitative program that allows operator manipulation to determine the site of greatest MCA as guided by the computer measurement of isotope count activity. The subsequent biopsy of these sites should optimally be accomplished with handheld probes to localize the site of MCA, although blind biopsies have also successfully localized the regions of interest.

The use of BEST imaging combines 2 fields of vascular abnormalities, cardiology and oncology, into a single diagnostic approach, which enhances the detection of breast cancer and distinguishes it from inflammatory changes of the breast and normal breast tissue by quantification of MCA resulting from differences in mitochondrial activity and blood flow. Although BEST imaging takes longer to complete than mammography, this study clearly demonstrates that BEST imaging is more accurate than mammography in distinguishing breast cancer from inflammatory changes of the breast or normal breast tissue, and can identify abnormalities as small as 4 mm.

References

1. American Heart Association. *Heart and Stroke Statistical Update.* American Heart Association; 1998. **PROVIDE THE LOCATION OF PUBLICATION**
2. The Health Network.com. Nov 16, 1999. **PROVIDE CORRECT WEB ADDRESS**
3. Burman ML, Taplin SH, Herta DF, Elmore JG. Effect of false-positive mammograms on interval breast cancer screening in a health maintenance organization. *Ann Intern Med.* 1999;131:1-6.
4. Fletcher SW. False-positive screening mammograms: good news, but more to do. *Ann Intern Med.* 1999;131:60-61.
5. Christiansen CL, Wang F, Barton MB, et al. Predicting the cumulative risk of false-positive mammograms. *J Natl Cancer Inst.* 200;92:1657-1666.

6. Rissanen TJ, Makarainen HP, Mattila SI, Lindholm EL, Heikkinen MI, Kiviniemi HO. Breast cancer recurrence after mastectomy: diagnosis with mammography and US. *Radiology*. 1993;188:463-467.
7. Eary JF. Nuclear medicine in cancer diagnosis. *Lancet*. 1999;354:853-857.
8. He J, Li Y, Su J. Differentiation of benign and malignant palpable breast masses using 99m Tc-MIBI imaging. *Hunan I Ko Ta Hsueh Hsueh Pao*. 1997;22:226-228.
9. Palmedo H, Biersack HJ, Lastoria S, et al. Scintimammography with technetium-99m methoxyisobutylisonitrile: results of a prospective European multicentre trial. *Eur J Nucl Med*. 1998;25:375-385.
10. Tilling R, Tatsch K, Sommer H, et al. Technetium-99m-sestamibi scintimammography for the detection of breast carcinoma: comparison between planar and SPECT imaging. *J Nucl Med*. 1998;39:849-856.
11. Salvatore M, Del Vecchio S. Dynamic imaging: scintimammography. *Eur J Radiol*. 1998;27:S259-S264.
12. Buscombe JR, Cwikla JB, Thakrar DS, Hilson AJ. Scintigraphic imaging of breast cancer: a review. *Nucl Med Commun*. 1997;18:698-709.
13. Cwikla JB, Buscombe JR, Barlow RV, et al. The effect of chemotherapy on the uptake of technetium-99m sestamibi in breast cancer. *Eur J Nucl Med*. 1997;24:1175-1178.
14. Cwikla JB, Buscombe JR, Kelleher SM, et al. Comparison of accuracy of scintimammography and X-ray mammography in the diagnosis of primary breast cancer in patients selected for surgical biopsy. *Clin Radiol*. 1998;53:274-280.
15. Amano S, Inoue T, Tomiyoshi K, Ando T, Endo K. In vivo comparison of PET and SPECT radiopharmaceuticals in detecting breast cancer. *J Nucl Med*. 1998;39:1424-1427.
16. Bombardieri E, Crippa F, Maffioli L, et al. Nuclear medicine approaches for detection of axillary lymph node metastasis. *Q J Nucl Med*. 1998;42(1):54-65.
17. Gulec SA, Moffat FL, Carroll RG, Krag DN. Gamma probe guided sentinel node biopsy in breast cancer. *Q J Nucl Med*. 1997;41:251-261.
18. Taillefer R, Robidoux A, Turpin S, Lambert R, Cantin J, Leveille J. Metastatic axillary lymph node technetium-99m-MIBI imaging in primary breast cancer. *J Nucl Med*. 1998;39:459-464.
19. Fleming RM, Dooley WC, Boyd LB, Kubovy K. Breast enhanced scintigraphy testing (BEST)—increased accuracy in detecting breast cancer accomplished by combining breast and cardiac imaging. Paper presented at: 48th Annual Scientific Session of the Society of Nuclear Medicine; Jun 27, 2001; Toronto, Ontario, Canada.
20. Fleming RM, Boyd L, Forster M. Angina is caused by regional blood flow differences—proof of a physiologic (not anatomic) narrowing. Paper presented at: Joint Session of the European Society–American College of Cardiology, ACC 49th Annual Scientific Sessions; Mar 12, 2000; Anaheim, CA.
21. Fleming RM. Regional blood flow differences induced by high dose dipyridamole explain etiology of angina. Paper presented at: 3rd International College of Coronary Artery Disease From Prevention to Intervention; Oct 4, 2000; Lyon, France.
22. Fleming RM. Nuclear cardiology: its role in the detection and management of coronary artery disease. In: Chang JC, ed. *Textbook of Angiology*. New York: Springer-Verlag; 1999:397-406.
23. Dooley WC. Endoscopic visualization of breast tumors. *JAMA*. 2000;284:1518.
24. Screening for breast cancer. Harvard Medical School Consumer Health Information. Feb 27, 2001. Available at www.intelihealth.com.
25. Fleming RM, Boyd LB, Kubovy C. Myocardial perfusion imaging using high dose dipyridamole defines angina: the difference between coronary artery disease (CAD) and coronary lumen disease (CLD). Paper presented at: 48th Annual Scientific Session of the Society of Nuclear Medicine; Jun 27, 2001; Toronto, Ontario, Canada.
26. Fleming RM, Dooley WC, Boyd LB, Kubovy C. Breast enhanced scintigraphy testing (BEST)—increased accuracy in detecting breast cancer accomplished by combining breast and cardiac imaging. Paper presented at: 48th Annual Scientific Session of the Society of Nuclear Medicine; Jun 26, 2001; Toronto, Ontario, Canada.
27. Fleming RM. The pathogenesis of vascular disease. In: Chang JC, ed. *Textbook of Angiology*. New York: Springer-Verlag; 1999:787-798.
28. Folkman J, Merler E, Abernathy C, Williams G. Isolation of a tumor factor responsible for angiogenesis. *J Exp Med*. 1971;133:275-288.
29. Stewart RJ, Panigraphy D, Flynn E, Folkman J. Vascular endothelial growth factor expression and tumor angiogenesis are regulated by androgens in hormone responsive human prostate carcinoma: evidence for androgen dependent destabilization of vascular endothelial growth factor transcripts. *J Urol*. 2001;165:688-693.